HHS Public Access

Author manuscript

ACS Nano. Author manuscript; available in PMC 2016 January 04.

Published in final edited form as:

ACS Nano. 2015 December 22; 9(12): 11800–11811. doi:10.1021/acsnano.5b05583.

Neutrophil-Mediated Delivery of Therapeutic Nanoparticles across Blood Vessel Barrier for Treatment of Inflammation and Infection

Dafeng Chu, **Jin Gao**, and **Zhenjia Wang***

Department of Pharmaceutical Sciences, College of Pharmacy, Washington State University, Spokane, Washington 99210, United States

Abstract

Endothelial cells form a monolayer in lumen of blood vessels presenting a great barrier for delivery of therapeutic nanoparticles (NPs) into extravascular tissues where most diseases occur, such as inflammation disorders and infection. Here, we report a strategy for delivering therapeutic NPs across this blood vessel barrier by nanoparticle *in situ* hitchhiking activated neutrophils. Using intravital microscopy of TNF-α-induced inflammation of mouse cremaster venules and a mouse model of acute lung inflammation, we demonstrated that intravenously (iv) infused NPs made from denatured bovine serum albumin (BSA) were specifically internalized by activated neutrophils, and subsequently, the neutrophils containing NPs migrated across blood vessels into inflammatory tissues. When neutrophils were depleted using anti-Gr-1 in a mouse, the transport of albumin NPs across blood vessel walls was robustly abolished. Furthermore, it was found that albumin nanoparticle internalization did not affect neutrophil mobility and functions. Administration of drug-loaded albumin NPs markedly mitigated the lung inflammation induced by LPS (lipopolysaccharide) or infection by *Pseudomonas aeruginosa*. These results demonstrate the use of an albumin nanoparticle platform for *in situ* targeting of activated neutrophils for delivery of therapeutics across the blood vessel barriers into diseased sites. This study demonstrates our ability to hijack neutrophils to deliver nanoparticles to targeted diseased sites.

Graphical abstract

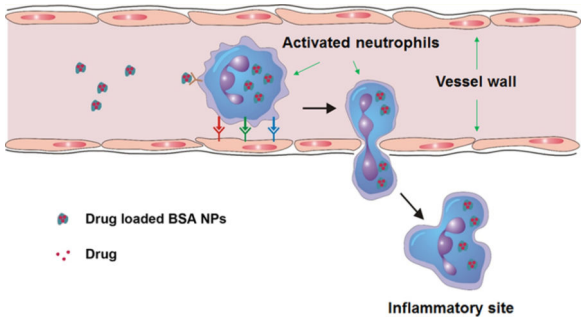

*Address correspondence to zhenjia.wang@wsu.edu.

Conflict of Interest: The authors declare no competing financial interest.

Keywords

nanoparticles; neutrophils; blood vessel; inflammation; infection

Targeted drug delivery and drug retention in extravascular diseased locations are prerequisites for pharmacological therapies and are also the primary goals of nanomedicine.[1–4] For medical benefit, therapeutic nanoparticles (NPs) should cross the blood vessel barrier.[1,5–7] However, current approaches are not sufficient in actively delivering NPs across this barrier. The endothelium forms a monolayer lining the vessel wall to regulate plasma permeability into tissues.[8] Generally, the physiological barrier of an interendothelial passage is smaller than 3 nm.[9] Therefore, the particles larger than this size are difficult to penetrate the endothelial gap into extravascular tissues. The EPR (enhanced permeation and retention) effect is often used for cancer targeting of drug delivery because leaky vessels could assist in the tissue deposition of therapeutic NPs. However, it is a passive process and particle-size dependent.[10]

Inflammation is the innate and adaptive immune responses characterized by a marked increase of immune cells and their trafficking from bloodstream to pathogenic tissues.[11,12] Millions of polymorphonuclear neutrophils, a type of white blood cells, can rapidly respond to inflammation through neutrophil activation, adhesion to and migration across endothelial vessels into inflammatory tissues *via* the intercellular route.[13,14] Therefore, neutrophils could be an excellent carrier to mediate the delivery of therapeutic NPs across the endothelial vessel barrier and to specifically target diseased tissues.

Nanotechnology has demonstrated to be a powerful tool to design nanotherapeutics which can incorporate therapeutic agents inside NPs and target desired cell types or organs by biologically functioning nanoparticle surfaces.[1,3] We have demonstrated that denatured albumin NPs can specifically target activated neutrophils adherent to the vessel wall using intravital microscopy of live mouse cremaster venules.[15] However, it is unknown whether these activated neutrophils can be exploited as a carrier to deliver nanoparticle cargo across the blood vessel barrier. Here, we hypothesized that therapeutic NPs could be delivered across the endothelial vessel wall using the neutrophil transmigration pathway (Figure 1A). The intravenously (iv) injected albumin NPs could be specifically internalized by activated neutrophils. Subsequently, the neutrophils containing NPs cross the blood vessel wall because neutrophils are able to transmigrate in response to inflammation induced by the pathogen invasion.[11–14] Using this strategy, we could deliver a range of therapeutics across the blood vessel barrier, improving therapies of various diseases originated from acute inflammation.

RESULTS AND DISCUSSION

Activated Neutrophils Transport Albumin NPs across Blood Vessel Barrier

To prove this concept, we first performed intravital microscopy of mouse cremaster venules to visualize in real-time whether neutrophils can transport albumin NPs across endothelial vessels into inflamed tissues. Two hours after intrascrotal injection of 0.5 μg TNF-α (tumor

necrosis factor), neutrophils were activated and adherent to the endothelium of cremaster venules, and were ready to migrate from bloodstream to inflamed tissues.[16] Thirty minutes after iv injection of both Alexa-Fluor-488-labeled mouse anti-Gr-1 to mark neutrophils[16] and bovine serum albumin (BSA) NPs conjugated with Cy5 (Cy5-BSA NPs) (the size is 130 nm, Figure S1A,B), we imaged the neutrophils in live mouse cremaster venules using intravital microscopy. The albumin NPs were internalized by adherent neutrophils and the neutrophils were moving into the muscle (Figure 1B and Movie 1). Thirty minutes later, we imaged again and found that some neutrophils containing NPs migrated across the vessels (Movie 2). The intravital images clearly demonstrated that activated neutrophils can transport albumin NPs across the blood vessel barrier.

In our recent studies, we physically incorporated fluorescent dyes in albumin NPs and found that the albumin NPs can be specifically internalized by activated neutrophils using intravital microscopy. The nanoparticle uptake is mediated *via* neutrophil Fcγ receptors interacting with denatured albumin after albumin nanoparticle formation.[15] When NPs were coated with natural albumin protein, neutrophils did not internalize the NPs. We also found that albumin nanoparticle uptake is independent of fluorescent labeling on their surface.[15] Here, we conjugated fluorescent dyes to BSA first and then mixed it with nonfluorescent BSA to fabricate albumin NPs showing the same neutrophil uptake as those of Cy5-loaded and Cy5 coated albumin NPs. Therefore, the nanoparticle uptake by neutrophils is mainly determined by denaturation of albumin rather than by fluorescent dyes. We characterized the size and zeta potential of albumin NPs made of fluorescently labeled albumin or loaded with drugs using dynamic light scattering (Figure S1A–C). The labeling and drug loading did not affect the properties of albumin NPs significantly. Moreover, the particle sizes did not change upon a series of dilution of NPs in 5% glucose and PBS, pH 7.4 (Figure S1D) and no free BSA was detected when the NPs were diluted in serum (Supporting Information), suggesting that our NPs are stable, which would be attributed to the fact that albumin protein was cross-linked after it formed a particle (see Methods).

To further confirm the finding that neutrophils can carry albumin NPs across the vessel barrier in a large tissue *in vivo*, we chose an acute lung inflammation model in mice. The lung has unique features with many tiny air sacs (called alveoli) surrounded by blood capillaries to form an interface between circulation and airspace.[17] When there is bacterial or viral infection in the airspace, neutrophils are capable of migrating from bloodstream to alveoli passing through the endothelial and epithelial barriers and accumulating in a distal lung airspace.[18,19] Therefore, the mouse model of acute lung inflammation is a novel system to further evaluate our hypothesis. Experimental scheme in the inset of Figure 1C shows our experiment design. Four hours after intratracheal (it) administration of lipopolysaccharide

Supporting Information Available: The Supporting Information is available free of charge on the ACS Publications website at DOI: 10.1021/acsnano.5b05583.

Stability of albumin NPs; characterizations of various NPs; flow cytometry of BALF and neutrophils in blood; confocal microscopy of neutrophils in BALF with PEG–PS NPs; numbers of leukocytes in BALF with blank NPs; HPLC chromatograph of BALF and plasma with TPCA-1 (PDF)

Movie 1 (AVI)

Movie 2 (AVI)

(LPS) (8 mg/kg) to the lung, neutrophils were activated and adherent to vessel walls, preparing to transmigrate into the lung airspace.[18,19] Afterward, we iv injected albumin NPs (the size is 130 nm, Figure S1) to the mouse. At 2, 10, and 20 h after nanoparticle injection, we collected lung bronchoalveolar lavage fluid (BALF) and blood. The cells were isolated and stained with mouse anti-Gr-1 antibody to mark neutrophils.[15] The confocal imaging (Figure 1C,D) showed that transmigrated neutrophils internalized albumin NPs and the number of neutrophils containing NPs temporally increased. To determine the percentage of lung infiltrated neutrophils which have internalized albumin NPs, we performed the flow cytometry to analyze the BALF collected at 2, 10, and 20 h after iv injection of NPs. In control, healthy mice (without LPS treatment) did not show the infiltration of neutrophils (Figure S2A). After LPS challenge, the cell population became primarily neutrophils, and the percentage of neutrophils increased with time (Figure S3). After iv injection of albumin NPs, the infiltrated neutrophils were divided to two populations: with and without the NPs (Figure 1E), but the percentage of totally infiltrated neutrophils was similar to the control (Figure S3) at each time point. Two hours after albumin nanoparticle injection, 6% of infiltrated neutrophils internalized albumin NPs and the number increased to 30% after 20 h (Figure 1F), which is consistent with the neutrophil transmigration process. At different time points, we also isolated neutrophils in peripheral blood in LPS-challenged mice, finding that the percentage of neutrophils containing the NPs decreased with time (Figure 1G and Figure S4). The finding that the percentage of NPs contained neutrophils decreased with time in blood, but accordingly, it increased in BALF (Figure 1F,G) is correlated with the neutrophil transmigration which mediates the transport of albumin NPs. To address whether activation of neutrophils is required for nanoparticle uptake, we administrated albumin NPs in healthy mice (without LPS challenge) *via* a tail vein. We found that resting neutrophils did not internalize albumin NPs (Figure 1G). The observation showed that only activated neutrophils (under inflammatory conditions) internalized the albumin NPs. This result was also demonstrated when we studied the uptake of albumin NPs by neutrophils in mouse cremaster venules using intravital microscopy.[15]

LPS-Induced Lung Permeability Does Not Contribute to the Transport of Albumin NPs into Lungs

To rule out the possibility that NPs would first pass through leaky vessels induced by LPS and then the infiltrated neutrophils internalize them in the lung airspace, we measured the concentrations of NPs in the plasma and BALF in a LPS-induced acute lung inflammation model. PEG-coated-yellow-green polystyrene NPs (PEG-coated NPs) were used as control and were produced with a similar size as albumin NPs (Figure S1). The protein influx into mouse lungs represents an increase of lung vessel permeability.[17] Therefore, we first studied a time course of lung permeability after LPS challenge and iv injection of albumin NPs or PEG-coated NPs by measuring the protein concentrations in BALF. The results indicated that the LPS challenge increased the lung permeability with time and the injection of NPs did not affect the lung permeability (Figure 2A). At 2, 10, and 20 h after injection of the PEG-coated NPs (Figure 2B) (Figure S2B for healthy mice and Figure S5 for the control without NPs), we found less than 1% of neutrophils containing PEG-coated NPs in BALF (Figure 2C), which is unlikely that PEG-coated NPs were internalized by neutrophils, as evident in the confocal imaging (Figure S6). We also studied the dynamics of PEG-coated

NPs and albumin NPs in the plasma and BALF. The PEG-coated NPs had much longer circulation than albumin NPs, which were even observed at 20 h after iv injection; however, the albumin NPs totally disappeared after 10 h (Figure 2D). In the BALF, the PEG-coated NPs were not detected at 2, 10, and 20 h after their injection, but the albumin NPs were observed at 10 and 20 h (Figure 2E). Consistent with the flow cytometry and confocal imaging (Figure 1), the results indicated that the transport of albumin NPs across lung blood vessel walls is an active process mediated by neutrophils rather than the nanoparticle diffusion through the leaky vasculature.

Neutrophil Depletion Abolishes the Delivery of Albumin NPs across Blood Vessel Barrier

To support the conclusion that neutrophils are a carrier to deliver albumin NPs across the blood vessel barrier, we performed the depletion of neutrophils using mouse anti-Gr-1 antibody.[20] To ensure the similar lung permeability between before and after the neutrophil depletion, we have optimized our experiments. Four hours after LPS challenge, we intraperitoneally (ip) injected anti-Gr-1 antibody and iv injected albumin NPs into mice. Twenty hours later, we measured the lung permeability. It was observed that the administration of anti-Gr-1 antibody did not significantly change the lung permeability induced by LPS (Figure 3A). When the number of neutrophils were counted, we found that the neutrophils in peripheral blood and BALF were depleted (Figure 3B). When albumin NPs in BALF were analyzed, they were not detected either; however, without injection of anti-Gr-1, the albumin NPs were observed in the BALF (Figure 3C). The result clearly demonstrated that albumin NPs accumulated in the lungs is mediated by the neutrophil transmigration pathway.

Uptake of Albumin NPs Does Not Change the Functions of Neutrophils

Next, we addressed whether the internalization of albumin NPs will affect the neutrophil mobility and activation. After injection of NPs (PEG-coated NPs or Cy5-BSA NPs), the number of infiltrated neutrophils (Figure 4A) and total leukocytes (Figure S7) did not significantly change compared with the control. Nanoparticle uptake also did not affect the cytokine release, such as IL-6 and TNF-α (Figure 4B,C), indicating that the nanoparticle internalization did not further promote the activation of neutrophils. Moreover, neutrophil uptake of albumin NPs did not alter the lung integrity because the protein concentration in lungs was similar to the PEG-coated NPs and the control (Figure 2A). Together, the results showed that neutrophils are a novel vehicle that chaperones albumin NPs across blood vessels and deposit them in targeted locations.

Increased Accumulation of Albumin NPs in Inflammatory Lungs

Although we have demonstrated that neutrophils are capable of mediating the delivery of albumin NPs into inflammatory lungs, it is not clear whether the accumulation of albumin NPs can be enhanced compared with that in healthy mice. After iv injection of albumin NPs in LPS-challenged mice, the albumin NPs mainly distributed in the liver, but they were also observed in the lung (Figure 5A). When we quantified the nanoparticle concentration ratio between lung and liver, we found that the ratio in LPS-challenged mice was significantly higher than that in healthy ones (Figure 5B). The result is consistent with the active delivery of albumin NPs mediated by the neutrophil transmigration.

TPCA-1-Loaded Albumin NPs Alleviate Acute Lung Inflammation/Injury

Acute lung injury (ALI), and its most severe form, acute respiratory distress syndrome (ARDS), cause 40% mortality in approximately 200 000 patients annually in the United States.[18,19] The pathological underlying of ALI is primarily linked to cytokine storms produced by resident lung macrophages.[21] The NF-κB pathway plays a central role in the production of cytokine storms.[22] Thus, we investigated whether neutrophils could mediate the delivery of albumin NPs loaded with a NF-κB inhibitor to improve the treatment of acute lung inflammation and injury.

To do so, we loaded TPCA-1 (2-[(aminocarbonyl)-amino]-5-(4-fluorophenyl)-3-thiophenecarboxamide),[23] a NF-κB inhibitor, into albumin NPs and quantified the TPCA-1 loading efficiency using high performance liquid chromatography (HPLC). The TPCA-1 concentrations in BALF and plasma were measured 20 h after injection of TPCA-1-loaded albumin NPs and free TPCA-1, respectively. It was found that TPCA-1 was detected in the BALF, but not in the plasma when mice were treated with TPCA-1-loaded albumin NPs (Figure 6A and Figures S8 and S9). In contrast, TPCA-1 was detected neither in the BALF nor in the plasma for TPCA-1 solution (Figure 6A and Figures S8 and S9). These results demonstrated that drug-loaded albumin NPs can be delivered across the blood vessel barrier and accumulate in the lung tissues.

To evaluate the therapeutic effect, we also compared inflammatory parameters (neutrophil infiltration and cytokine release (IL-6 and TNF-α)) after the treatment with TPCA-1-loaded albumin NPs with those after the administration of free drug solution (Figure 6B–D). The results indicated that the TPCA-1-loaded albumin NPs dramatically attenuated the lung inflammation (Figure 6B–D) and lowered the lung permeability compared with the free drug (Figure 6E), representing that the albumin NPs can improve the lung integrity to prevent lung edema.[17]

Antibiotic-Loaded Albumin NPs Impair Bacterial Infection

Pseudomonas aeruginosa is one of the most recalcitrant pathogens and a leading cause of acute pneumonia.[24] Thus, there is a need to specifically target the pathogenic locations, such as in the lung. Using the albumin NPs loaded with cefoperazone acid (Cefo-A), a broad-spectrum antibiotic,[25] we examined whether the treatment of lung infection could be improved. In control experiments, the leukocyte infiltration, inflammation factors (IL-6 and TNF-α), and lung permeability were analyzed after iv injection of the Cefo-A loaded albumin NPs in the mice with LPS-induced lung inflammation. The comparison with vehicle group of 5% glucose showed that the Cefo-A-loaded albumin NPs did not affect the neutrophil mobility and activation and the lung integrity (Figure 7A,B). Furthermore, Cefo-A-loaded albumin NPs did not attenuate lung inflammation (Figure 7C,D). The results suggested that Cefo-A-loaded albumin NPs did not affect the functions of neutrophils and inflammatory response of the mice to LPS challenge. Cefo-A does not have the anti-inflammatory effect, so it is not surprising that we did not observe the impairment of inflammation induced by LPS after the administration of Cefo-A-loaded albumin NPs.

When delivering the Cefo-A-loaded albumin NPs in *P. aeruginosa*-infected lungs, we observed that the NPs dramatically declined bacterial proliferation by three folds compared with free Cefo-A in solution (Figure 7E). These results further proved the concept of neutrophils as a carrier to mediate the delivery of therapeutic agents into targeted tissues.

CONCLUSION

In summary, we have demonstrated the use of *in situ* targeting activated neutrophils using albumin NPs for drug delivery applications. With this approach, activated neutrophils are capable of mediating the delivery of therapeutic albumin NPs across the blood vessel barrier into inflammation sites, thus dramatically alleviating acute lung inflammation/injury induced by LPS and lung infection by *P. aeruginosa*. Human neutrophils account for 50–70% of all circulating leukocytes;[26] thus, we expect that our drug delivery platform would have a great impact on treatment of a wide range of inflammatory diseases and infections. Most importantly, our findings reveal a new strategy for designing nanotherapeutics which are capable of *in situ* hitchhiking neutrophils for targeted drug delivery.

METHODS

Materials

Lipopolysaccharide (LPS), bovine serum albumin (BSA) and BMS-345541 were purchased from Sigma (St. Louis, MO). Cefoperazone acid (Cefo-A) was obtained from Santa Cruz Biotechnology (Dallas, TX). Glutaraldehyde was obtained from Electron Microscopy Sciences (Hatfield, PA). Alexa Fluor-488 and Alexa Fluor-647-labeled anti-mouse Gr-1(Ly-6G/Ly-C6) and Ultra-LEAF Purified anti-mouse Ly-6G/Ly-6C (Gr-1) antibody (Clone: RB6-8C5) were purchased from Biolegend (San Diego, CA). Carboxylated polystyrene fluorescent yellow-green NPs (100 nm in a diameter; 2%, w/v; excitation/emission: 505 nm/515 nm) were purchased from Invitrogen (Grand Island, NY). EDC (1-ethyl-3-(3-(dimethylamino)propyl)carbodiimide) and sulfo-NHS (*N*-hydroxysulfo succinimide) were purchased from Pierce (Rockford, IL). mPEG-NH_2 (5000 Da) was purchased from Laysan Bio (Arab, AL). MES ((2-*N*-morpholino)ethanesulfonic acid) was from Fisher Scientific (Pittsburgh, PA). TPCA-1 was from Medchemexpress (Monmouth Junction, NJ). Freeze-dried *P. aeruginosa* (ATCC 29260) was obtained from ATCC (Manassas, VA).

Preparation of Cy5-BSA NPs and TPCA-1 or Cefoperazone Acid Loaded BSA NPs (TPCA-1 or Cefo-A BSA NPs)

BSA was labeled with Cy5 NHS ester (Lumiprobe, Hallandale Beach, FL) according to manufacturer's protocol. Cy5-BSA NPs (Cy5-BSA/BSA, 1:1, w/w) were prepared by the desolvation technique.[15] BSA was first dissolved at the concentration of 20 mg/mL in deionized water. Afterward, 0.2 mL DMSO was added to 1 mL of the BSA solution, which was stirred at 1600 rpm. Fifteen minutes later, the solution was quickly mixed with 3.5 mL of ethanol under stirring (600 rpm) at room temperature. To make TPCA-1 or Cefo-A BSA NPs, 1 mL of 20 mg/mL BSA solution was incubated with 4 mg of TPCA-1 or 0.5 mg Cefo-A dissolved in 0.2 mL of DMSO for 15 min, and then mixed with 3.5 mL of ethanol. To

form stable albumin NPs with or without drug, 1 h later BSA molecules were cross-linked by adding 80 μL of 2% glutaraldehyde into the suspension. The suspension was stirred overnight at room temperature and centrifuged at 20 000*g* for 30 min at 4 °C. The nanoparticle pellet was centrifuged three times to remove organic solvents and the unencapsulated drug, and then was resuspended in water or 5% glucose for experiments.

To measure the drug content of BSA NPs, the concentrations of TPCA-1 or Cefo-A were determined by a Waters HPLC with 2690 Separations Module, 486 UV detector and Ultra C18 column, 4.6 × 250 mm, 5 μm (Restek, Bellefonte, PA). The flow rate was 1 mL and the injection volume was 5 μL. For TPCA-1, the mobile phase was methanol/water, 65:35 (v/v) and the detection wavelength was 310 nm. The standards were prepared in methanol and the linear range was between 1 and 25 μg/mL (R = 0.999). For Cefo-A, The initial mobile phase was methanol/0.005% acetic acid aqueous solution, 10: 90 (v/v), which gradually changed to 90:10 (v/v) at 10 min. At 10.01 min, the ratio of methanol/aqueous solution was decreased to 10% for 5 min. The standards were prepared in deionized water and the linear range was between 1 and 25 μg/mL(R = 0.999). Furthermore, NPs suspension was dried by lyophilization and weighed. The drug content of TPCA-1 in NPs was calculated with the following equation: drug content = (drug used − unloaded drug)/dried BSA NPs. Finally, we obtained BSA NPs containing 25 ± 1.3 wt% of TPCA-1 and 3.2 ± 0.3 wt% of Cefo-A, respectively. The particle sizes were measured by Malvern Zetasizer Nano ZS90 (Westborough, MA).

Preparation of PEG–Polystyrene NPs (PEG–PS NPs)

To covalently conjugate mPEG-NH_2 5k to polystryrene COOH-NPs (PS COOH-NPs), we used the carboxyl-amine reaction.[7] The COOH groups on PS NPs were first activated. In detail, 0.3 mL of original particle solution (20 mg/mL) in 2.7 mL of MES buffer (50 mM, pH = 6) was mixed with 75 μL of EDC (80 mg/mL) and 75 μL of sulfo-NHS (160 mg/mL) for reaction of 15 min. The mixture was washed with PBS buffer (pH = 7.4) and centrifuged using Amicon Ultra-4 100k Centrifugal Filter Units (EMD Millipore, Billerica, MA) three times. After activation of NPs, we added 3 mL of 20 mg/mL mPEG-NH_2 solution to the activated particle solution and allowed them to react for 2 h in room temperature. The mixture was washed with 5% glucose and centrifuged three times using the same Filter Units as described above. After reaction, the particle sizes increased from 109 to 116.7 nm and the zeta potentials decreased from −40.7 to −27.7 mV in terms of PS COOH-NPs and PS PEG-NPs, indicating that we successfully conjugated PEG molecules to NPs.

Mice

Adult CD1 mice (22–26 g, 4–5 weeks) were purchased from Harlan Laboratories (Madison, WI). The mice were maintained in polyethylene cages with stainless steel lids at 20 °C with a 12 h light/dark cycle and covered with a filter cap. Animals were fed with food and water *ad libitum*. The Washington State University Institutional Animal Care and Use Committee approved all animal care and experimental protocols used in these studies. All experiments were made under anesthesia using intraperitoneal (ip) injection of the mixture of ketamine (120 mg/kg) and xylazine (6 mg/kg) in saline.

Intravital Microscopy of Live Mouse Cremaster Venules

Using intravital microscopy, we can visualize in real-time that neutrophils take up albumin NPs and transport them across endothelial vessel walls moving to inflammation sites in live mouse cremaster venules.[15] TNF-α (500 ng in 250 μL saline) was intrascrotally injected into the mice. At 2 h after TNF-α injection, the mice were anesthetized with ip injection of a mixture of ketamine (120 mg/kg) and xylazine (6 mg/kg), and maintained at 37 °C on a thermo-controlled rodent blanket. A tracheal tube was inserted and a right jugular vein was cannulated for injection of NPs, antibodies or drugs. After the scrotum was incised, the testicle and surrounding cremaster muscles were exteriorized onto an intravital microscopy tray. The cremaster preparation was perfused with thermo-controlled (37 °C) and aerated (95% N_2, 5% CO_2) bicarbonate-buffered saline throughout the experiment. Images were recorded using a Nikon A1R$^+$ laser scanning confocal microscope with a resonant scanner. To study neutrophil uptake of albumin NPs, 30 min after iv injection of Alexa Fluor 488-labled Gr-1 antibody (1.5 μg/mouse) and Cy5-BSA NPs (80 μg/mouse) into the TNF-α-treated mouse, water immersion objective with NA = 1.1 was used to image cremaster venules. Two lasers at 488 and 640 nm simultaneously excited cremaster tissues to image neutrophils and albumin NPs at 10 frames/s for 512 × 512 pixels. Images were analyzed using Nikon software.

LPS Challenge and Neutrophils Depletion

After the mice were anesthetized, they were placed in a supine position head up on a board tilted at 15°. Afterward, 8 mg/kg of LPS from *Escherichia coli* (serotype 0111.B4, Sigma-Aldrich, St. Louis, MO) in 50 μL of Hank's Balanced Salt Solution (HBSS) was nebulized into the pulmonary alveoli with a FMJ-250 High Pressure Syringe (Penn-Century, Wyndmoor, PA). Mice were held upright for 2 min after the administration. For neutrophil depletion, after LPS challenge, the mice were ip injected with 0.5 mg of Ultra-LEAF Purified anti-mouse Ly-6G/Ly-6C (Gr-1) antibody.

Bronchoalveolar Lavage Fluid (BALF), Blood, Plasma, and Organs Collection

Four hours after LPS challenge, 200 μL of 16 mg/kg of PEG–PS NPs in 5% glucose, 16 mg/kg of Cy5-BSA NPs in 5% glucose, 16 mg/kg of Cy5-BSA NPs in 5% glucose + neutrophils depletion, 8 mg/kg of TPCA-1 in 5% DMSO (v/v), 10% Tween 20 (v/v), 5% glucose solution or TPCA-1 BSA NPs with TPCA-1 at 8 mg/kg in 5% glucose were iv injected into the mice *via* tail vein, respectively. At predetermined time points, mouse BAL fluid (BALF) was collected by inserting a needle into the upper trachea. Cefo-A BSA NPs with Cefo-A at 25 mg/kg in 200 μL 5% glucose were iv injected to the mice at 12 h after LPS challenge. BALF was then harvested at 12 h after NPs were administered. Lavage was performed by introducing three sequential 0.9 mL of HBSS into the lungs and BALF was carefully withdrawn.[27] The BALF was centrifuged at 350*g* for 10 min. The supernatant of BALF was collected and stored at −20 °C. Cells were resuspended in 1 mL of red blood cell (RBC) lysis buffer (Qiagen Sciences, Germantown, MD) for 30 min at room temperature. The cell suspensions were then washed with 1 mL of HBSS and centrifuged for three times. Afterward, the cell suspensions were resuspened in 200 μL of HBSS for the quantitation of PEG–PS NPs and Cy5-BSA NPs in the cells. In different groups, the cell pellet was

resuspended in 1 mL of HBSS, 10 μL of which was employed for counting the number of cells in a hemocytometer and 200 μL of which was used to prepare the slide smears by 7620 Cytopro Cytocentrifuge (ELITech, Princeton, NJ). The smears were stained with Differential Quick Stain Kit (Polysciences, Warrington, PA), and then, leukocytes and neutrophils were quantified under a microscope. Afterward, the cell suspension was concentrated to 400 μL for flow cytometry and confocal microscopy. Blood was collected into the heparin tubes by cardiac puncture. The neutrophils in blood were isolated by Pluriselect anti-mouse-Ly6G S-pluribeads according to the manufacturer's protocol (Pluriselect, Spring Valley, CA). The plasma was harvested and stored at −20 °C after the blood was centrifuged at 1500*g* for 20 min. After the depletion of neutrophils, blood was also treated with RBC lysis buffer and subject to hemocytometer and Differential Quick Stain Kit. After the administration of the Cy5-BSA NPs, various organs were collected from the mice with and without LPS challenge and stored at −80 °C.

Determination of NPs in BALF, Plasma, Blood, and Organs

The concentrations of PEG–PS NPs (excitation 485 nm and emission 515 nm) in BALF supernatant, BALF cells and plasma, and the concentrations of Cy5-BSA NPs (excitation 645 nm and emission 675 nm) in BALF supernatant, BALF cells, plasma, blood and various organs were measured by Synergy Neo fluorescence plate reader (BioTek, Winooski, VT). For PEG–PS NPs and Cy5-BSA NPs in BALF and plasma, standards were prepared by adding the NPs to BALF supernatant, BALF cells in 200 μL of HBSS after the treatment of RBC lysis buffer and plasma collected from the mice 2, 10, and 20 h after LPS challenge without the administration of NPs. The linear range was from 0.02 to 1 μg/mL $R = 0.989$) for PEG-PS NPs and 0.04 to 6 μg/mL ($R = 0.992$) for Cy5-BSA NPs in BALF supernatant and cells. In plasma, the linear range was between 0.2 and 1 μg/mL ($R = 0.991$) for PEG-PS NPs and 0.8 to 6 μg/mL ($R = 0.993$) for Cy5-BSA NPs. In blood, standards were prepared by adding the Cy5-BSA NPs to blood collected from the mice 20 h after LPS challenge without the administration of NPs. The linear range was between 1 and 10 μg/mL ($R = 0.985$) for Cy5-BSA NPs. In terms of Cy5-BSA NPs in various organs, standards were prepared by adding the Cy5-BSA NPs to the blank organ collected from the mice at 20 h with or without LPS challenge. Afterwards, the organs were homogenized with 4 parts (w/w) of PBS buffer to obtain the pipettable homogenate. Finally, 100 mg of the homogenate was subject to the fluorescence measurement mentioned above with the linear range of 4–100 μg/mL ($R = 0.988$). Samples were diluted when they were beyond the calibration range.

Determination of TPCA-1 in BALF and Plasma

Both 25 μL of various TPCA-1 solutions and 25 μL of 4 μg/mL BMS 345541 internal standard solution in methanol were added to 300 μL of plasma or 500 μL of BALF from the mice 20 h after LPS challenge without the administration of NPs. In terms of the plasma and BALF samples from the mice administered with TPCA-1 NPs, only 50 μL of methanol was added. The samples were then vortexed for 0.5 min before 2 mL of chloroform was added. After the tubes were vortexed for 5 min, they were centrifuged at 3000*g* for 20 min. Afterward, organic layers were transferred to clean tubes and evaporated to dryness at room temperature under a stream of air. Residues were reconstituted in 50 μL of methanol/

0.0025%(v/v) acetic acid aqueous solution, 30:70 (v/v), which were briefly vortex-mixed and then 20 μL was injected into the HPLC system with the same flow rate and detection wavelength as described previously. The initial mobile phase was methanol/0.0025% acetic acid aqueous solution, 30:70 (v/v), which gradually changed to 90:10 (v/v) at 8 min. At 10.01 min, the ratio of methanol/aqueous solution was decreased to 30% for 5 min. Quantitation of TPCA-1 was based on calibration curves of peak area ratio (drug/internal standard) *versus* concentration.

Determination of IL-6, TNF-α and Total Protein in BALF

The concentrations of IL-6 and TNF-α in BALF were determined with ELISA MAX Deluxe Sets (Biolegend, San Diego, CA) and the protein in BALF was measured by Pierce BCA protein Assay Kit (Thermo Scientific, Rockford, IL) according to manufacturer's protocol.

Flow Cytometry

The neutrophils from blood and the BALF cells were washed with 3 mL of 5% BSA HBSS and centrifuged at 350*g* for 5 min three times, which was finally resuspended in 400 μL of 5% BSA HBSS. The cell suspension was incubated with 1 μg of Alexa Fluor 488-conjugated anti-mouse Gr-1 antibody for Cy5-BSA NPs groups and Alexa Fluor-647-labeled anti-mouse Gr-1 antibody for PEG–PS NPs groups in the dark for 20 min, followed by washing with 3 mL of 0.1% BSA HBSS under centrifugation for three times. Cells were then resuspended in 400 μL of 0.1% BSA HBSS and analyzed by Accuri C6 flow cytometer (BD Biosciences, San Jose, CA).

Confocal Microscope

The cell suspensions were fixed with 2 mL of 4% paraformaldehyde overnight, which was then resuspended in 200 μL of HBSS. Smears on slide were prepared by the same methods as described above. After one drop of Prolong Gold antifade reagent with DAPI (Invitrogen, Eugene, OR) was added on the cells, a cover slide was applied. Four hours later, the cells were observed by Olympus Fluoview FV1000 confocal microscope (Center Valley, PA).

P. aeruginosa Culture

The freeze-dried bacteria were streaked on the sheep blood agar plates (Hardy Diagnostics, Santa Maria, CA) and grown at 37 °C for 15 h in an incubator. The bacteria were then scratched from the plate and resuspended in PBS, pH 7.4. The concentrations of bacteria were determined by counting colony forming units (cfu) of diluted bacteria suspension on the sheep blood agar plates after incubation 37 °C for 15 h.

Lung Infection of *P. aeruginosa*

Anesthetized mice were first placed in a supine position head up on a board tilted at 15°, and then 1×10^6 cfu of *P. aeruginosa* in 40 μL of PBS, pH 7.4 were instilled to the trachea.[24] Mice were held upright for 2 min after the administration.

Bacteriological Assessment of BALF of Infected Lungs

Twelve hours after *P. aeruginosa* infection, 200 μL of Cefo-A solution of 5% DMSO(v/v), 10% Tween 20 (v/v), and 5% glucose (w/v) (25 mg/kg) or Cefo-A BSA NPs in 5% glucose with Cefo-A at 25 mg/kg was injected *via* tail vein. The BALF was collected 12 h after the drug administration as mentioned above. The cfu of *P. aeruginosa* in BALF was counted on the sheep blood agar plates after incubation 37 °C for 15 h.

Statistical Analysis

Data were expressed as mean ± SD or SEM. Statistical analysis was conducted using two-sample Student's *t*-test of Origin 8.5, p values < 0.05 were considered significant.

Supplementary Material

Refer to Web version on PubMed Central for supplementary material.

Acknowledgment

The work was supported by NIH Grant K25HL111157 and WSU startup to Z.W.

REFERENCES AND NOTES

1. Farokhzad OC, Langer R. Impact of Nanotechnology on Drug Delivery. ACS Nano. 2009; 3:16–20. [PubMed: 19206243]
2. Rodriguez PL, Harada T, Christian DA, Pantano DA, Tsai RK, Discher DE. Minimal "Self" Peptides That Inhibit Phagocytic Clearance and Enhance Delivery of Nanoparticles. Science. 2013; 339:971–975. [PubMed: 23430657]
3. Torchilin VP. Multifunctional, Stimuli-Sensitive Nanoparticulate Systems for Drug Delivery. Nat. Rev. Drug Discovery. 2014; 13:813–827. [PubMed: 25287120]
4. Mitragotri S, Burke PA, Langer R. Overcoming the Challenges in Administering Biopharmaceuticals: Formulation and Delivery Strategies. Nat. Rev. Drug Discovery. 2014; 13:655–672. [PubMed: 25103255]
5. Wang Z, Malik AB. Nanoparticles Squeezing across the Blood-Endothelial Barrier *Via* Caveolae. Ther. Delivery. 2013; 4:131–133.
6. Wang Z, Tiruppathi C, Cho J, Minshall RD, Malik AB. Delivery of Nanoparticle: Complexed Drugs across the Vascular Endothelial Barrier *Via* Caveolae. IUBMB Life. 2011; 63:659–667. [PubMed: 21766412]
7. Wang Z, Tiruppathi C, Minshall RD, Malik AB. Size and Dynamics of Caveolae Studied Using Nanoparticles in Living Endothelial Cells. ACS Nano. 2009; 3:4110–4116. [PubMed: 19919048]
8. Komarova Y, Malik AB. Regulation of Endothelial Permeability *Via* Paracellular and Transcellular Transport Pathways. Annu. Rev. Physiol. 2010; 72:463–493. [PubMed: 20148685]
9. Mehta D, Malik AB. Signaling Mechanisms Regulating Endothelial Permeability. Physiol. Rev. 2006; 86:279–367. [PubMed: 16371600]
10. Schroeder A, Heller DA, Winslow MM, Dahlman JE, Pratt GW, Langer R, Jacks T, Anderson DG. Treating Metastatic Cancer with Nanotechnology. Nat. Rev. Cancer. 2012; 12:39–50. [PubMed: 22193407]
11. Dinarello CA. Anti-Inflammatory Agents: Present and Future. Cell. 2010; 140:935–950. [PubMed: 20303881]
12. Medzhitov R. Inflammation 2010: New Adventures of an Old Flame. Cell. 2010; 140:771–776. [PubMed: 20303867]
13. Kolaczkowska E, Kubes P. Neutrophil Recruitment and Function in Health and Inflammation. Nat. Rev. Immunol. 2013; 13:159–175. [PubMed: 23435331]

14. Jenne CN, Wong CH, Zemp FJ, McDonald B, Rahman MM, Forsyth PA, McFadden G, Kubes P. Neutrophils Recruited to Sites of Infection Protect from Virus Challenge by Releasing Neutrophil Extracellular Traps. Cell Host Microbe. 2013; 13:169–180. [PubMed: 23414757]
15. Wang Z, Li J, Cho J, Malik AB. Prevention of Vascular Inflammation by Nanoparticle Targeting of Adherent Neutrophils. Nat. Nanotechnol. 2014; 9:204–210. [PubMed: 24561355]
16. Sumagin R, Prizant H, Lomakina E, Waugh RE, Sarelius IH. Lfa-1 and Mac-1 Define Characteristically Different Intralumenal Crawling and Emigration Patterns for Monocytes and Neutrophils *in Situ*. J. Immunol. 2010; 185:7057–7066. [PubMed: 21037096]
17. Ware LB, Matthay MA. Clinical Practice. Acute Pulmonary Edema. N. Engl. J. Med. 2005; 353:2788–2796. [PubMed: 16382065]
18. Matthay MA, Ware LB, Zimmerman GA. The Acute Respiratory Distress Syndrome. J. Clin. Invest. 2012; 122:2731–2740. [PubMed: 22850883]
19. Matthay MA, Zemans RL. The Acute Respiratory Distress Syndrome: Pathogenesis and Treatment. Annu. Rev. Pathol.: Mech. Dis. 2011; 6:147–163.
20. Czuprynski CJ, Brown JF, Maroushek N, Wagner RD, Steinberg H. Administration of Anti-Granulocyte Mab Rb6–8c5 Impairs the Resistance of Mice to Listeria Monocytogenes Infection. J. Immunol. 1994; 152:1836–1846. [PubMed: 8120393]
21. Chow CW, Herrera Abreu MT, Suzuki T, Downey GP. Oxidative Stress and Acute Lung Injury. Am. J. Respir. Cell Mol. Biol. 2003; 29:427–431. [PubMed: 14500253]
22. Strnad J, Burke JR. Ikappab Kinase Inhibitors for Treating Autoimmune and Inflammatory Disorders: Potential and Challenges. Trends Pharmacol. Sci. 2007; 28:142–148. [PubMed: 17287032]
23. Podolin PL, Callahan JF, Bolognese BJ, Li YH, Carlson K, Davis TG, Mellor GW, Evans C, Roshak AK. Attenuation of Murine Collagen-Induced Arthritis by a Novel, Potent, Selective Small Molecule Inhibitor of Ikappab Kinase 2, Tpca-1 (2-[(Aminocarbonyl)Amino]-5-(4-Fluorophenyl)-3-Thiophenecarboxamide), Occurs *Via* Reduction of Proinflammatory Cytokines and Antigen-Induced T Cell Proliferation. J. Pharmacol. Exp. Ther. 2005; 312:373–381. [PubMed: 15316093]
24. Sadikot RT, Zeng H, Joo M, Everhart MB, Sherrill TP, Li B, Cheng DS, Yull FE, Christman JW, Blackwell TS. Targeted Immunomodulation of the Nf-Kappab Pathway in Airway Epithelium Impacts Host Defense against *Pseudomonas Aeruginosa*. J. Immunol. 2006; 176:4923–4930. [PubMed: 16585588]
25. Jacqueline C, Roquilly A, Desessard C, Boutoille D, Broquet A, Le Mabecque V, Amador G, Potel G, Caillon J, Asehnoune K. Efficacy of Ceftolozane in a Murine Model of *Pseudomonas Aeruginosa* Acute Pneumonia: In Vivo Antimicrobial Activity and Impact on Host Inflammatory Response. J. Antimicrob. Chemother. 2013; 68:177–183. [PubMed: 22941899]
26. Mayadas TN, Cullere X, Lowell CA. The Multifaceted Functions of Neutrophils. Annu. Rev. Pathol.: Mech. Dis. 2014; 9:181–218.
27. Wang YL, Malik AB, Sun Y, Hu S, Reynolds AB, Minshall RD, Hu G. Innate Immune Function of the Adherens Junction Protein P120-Catenin in Endothelial Response to Endotoxin. J. Immunol. 2011; 186:3180–3187. [PubMed: 21278343]

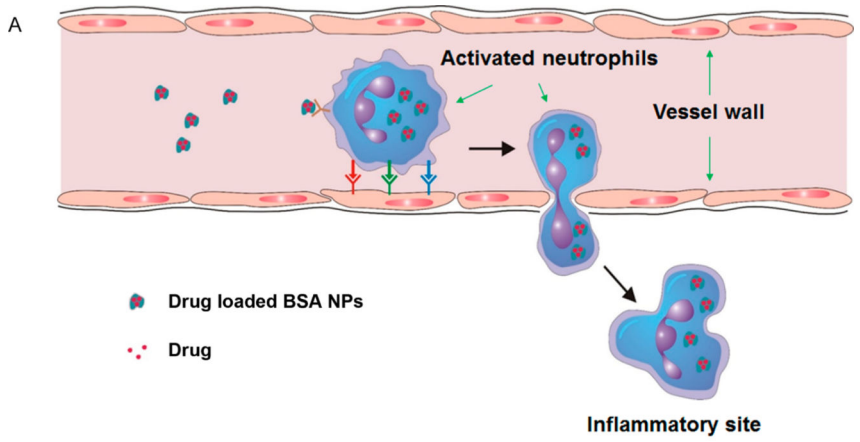

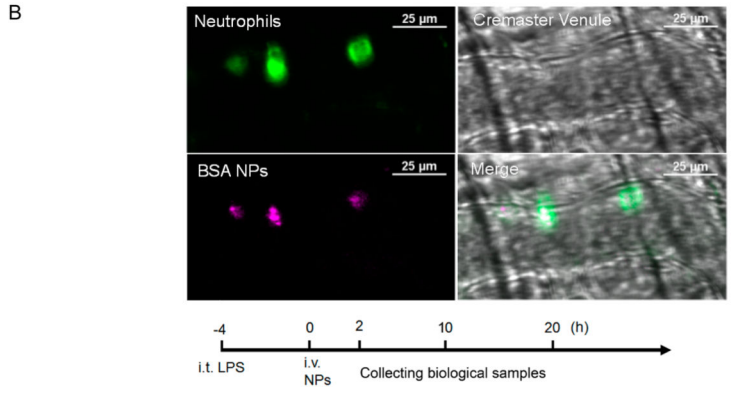

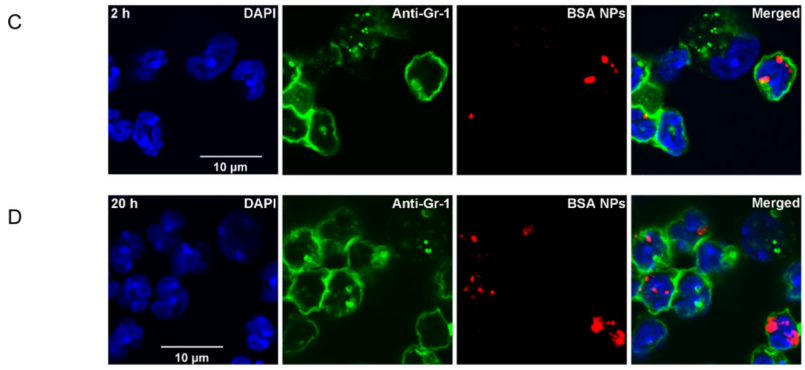

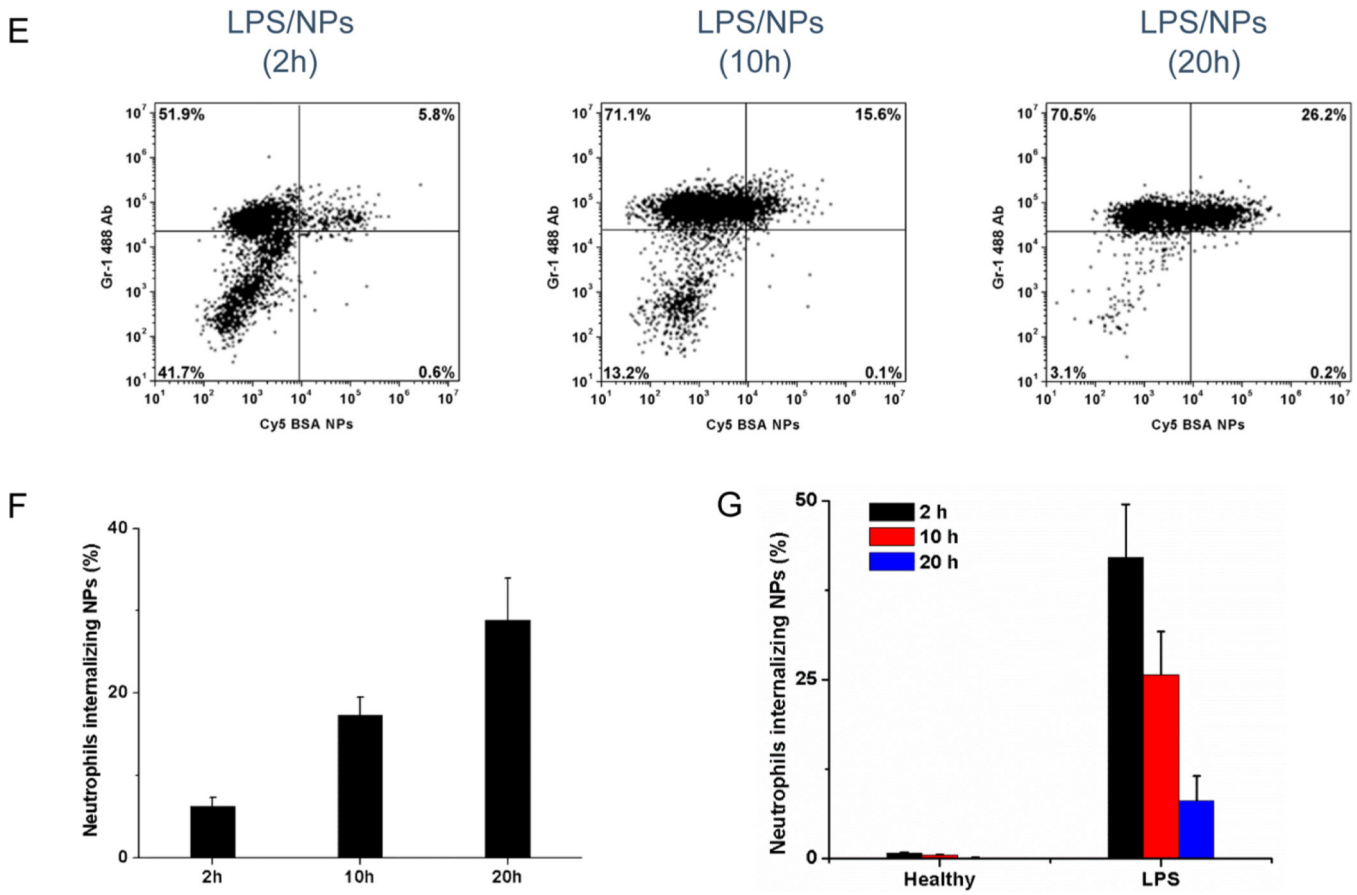

Figure 1.

Neutrophils mediate delivery of albumin nanoparticles across blood vessel barrier moving to inflammation sites. (A) The concept of neutrophil-mediated delivering of therapeutic albumin NPs. (B) Intravital microscopic images of TNF-α-induced inflammation of live mouse cremaster venules, 30 min after intravenous (iv) injection of Cy5-BSA NPs (80 μg/mouse) and Alexa Fluor-488-labeled anti-mouse Gr-1 (1.5 μg/mouse) to mark neutrophils (green). Fluorescence confocal microscopy of neutrophils from bronchoalveolar lavage fluid (BALF) 2 h (C) and 20 h (D) after iv injection of Cy5-BSA NPs (red) (neutrophils were labeled by Alexa Fluor 488-labeled anti-mouse Gr-1 antibody, green). Nucleus were stained by DAPI (blue). The diagram above panels C and D shows the experimental protocol of mouse acute lung inflammation. (E) Flow cytometry of BALF after iv injection of Cy5-BSA NPs. Neutrophils were stained as described above. (F) Percentage of neutrophils internalizing NPs in BALF, obtained from flow cytometry. (G) Percentage of neutrophils internalizing NPs in blood of mice challenged with and without LPS, obtained from flow cytometry. A total of 16 mg/kg of NPs was administered in mice 4 h after LPS challenge (8 mg/kg). All data represent means ± SD (n = 3–4 mice per group).

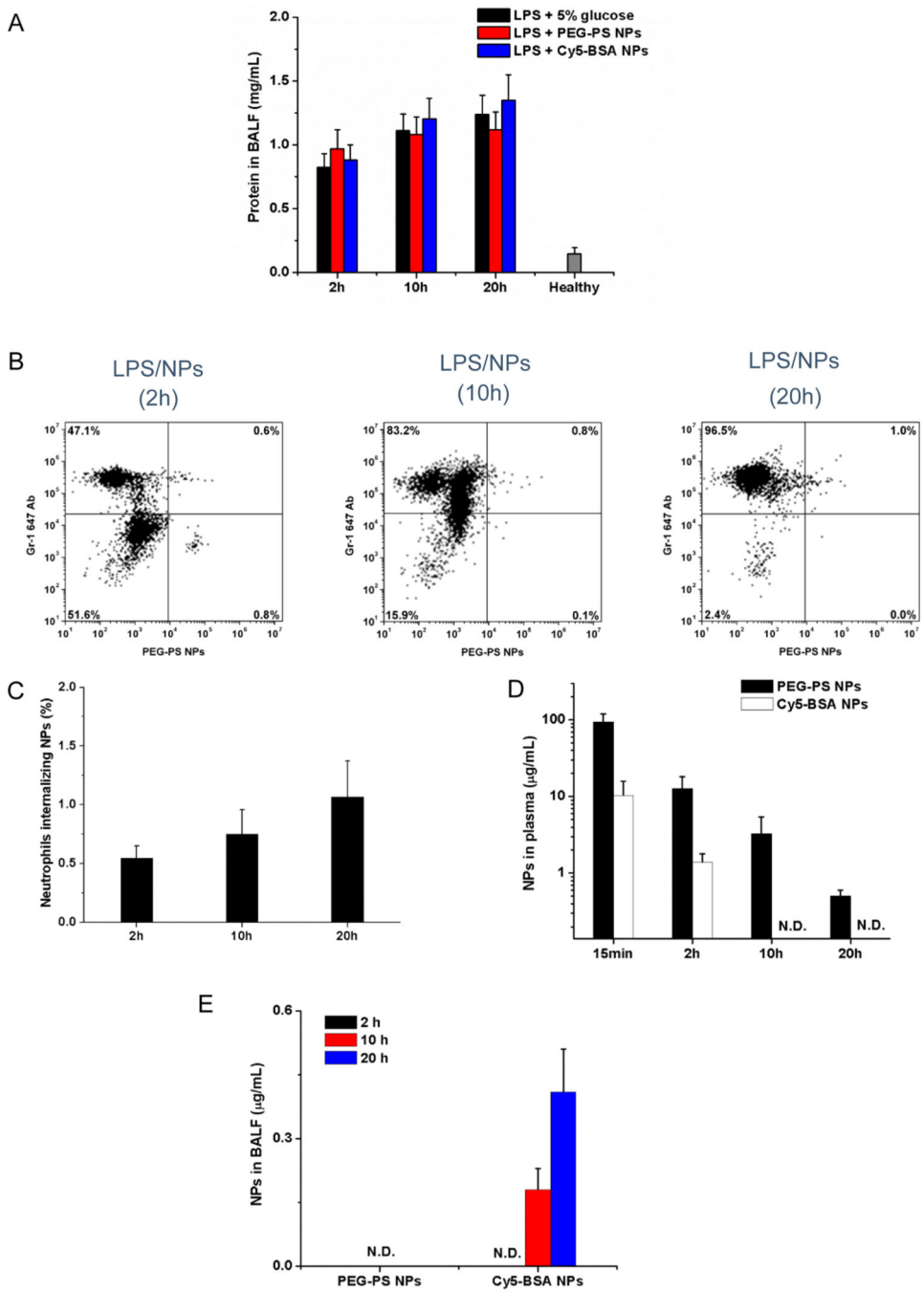

Figure 2.

LPS-induced lung permeability does not contribute transport of albumin NPs across blood vessel barrier. (A) Concentrations of proteins in BALF after iv injection of 5% glucose, Cy5-BSA NPs, or PEG–PS NPs in mice 4 h after LPS challenge. (B) Flow cytometry of neutrophils in BALF after the administration of PEG–PS NPs in mice 4 h after LPS challenge (neutrophils were labeled by Alexa Fluor 647-labeled anti-mouse Gr-1 antibody). The protocol described as in Figure 1E. (C) Percentage of neutrophils internalizing NPs in BALF, obtained from flow cytometry. Concentrations of NPs in plasma (D) and BALF (E)

after iv injection of NPs (16 mg/kg). NPs were administered in mice 4 h after LPS challenge (8 mg/kg). All data represent means ± SD (n = 3–4 mice per group). N.D., not detected.

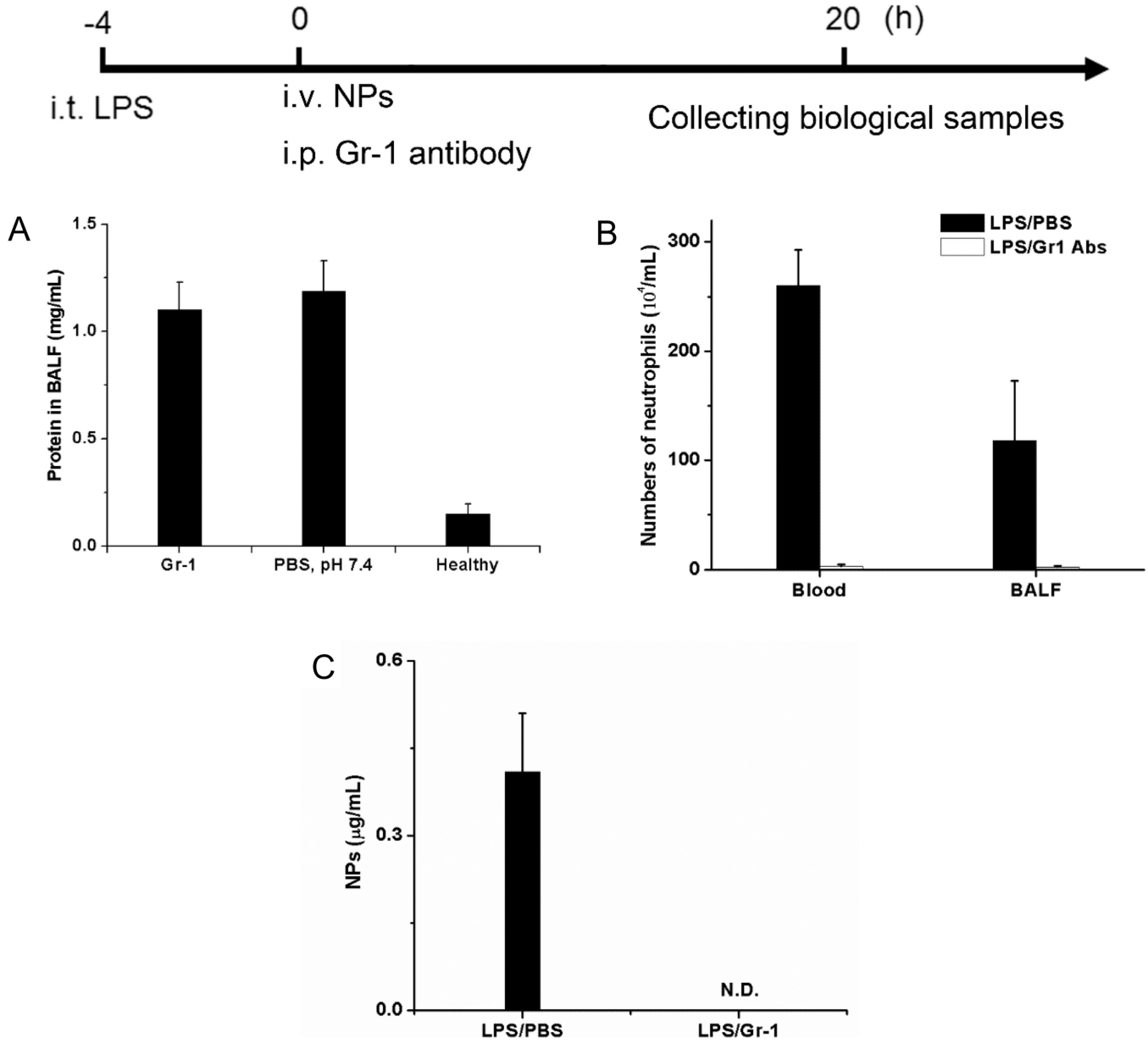

Figure 3.

Neutrophil depletion prevents the delivery of albumin NPs across blood vessel barrier. The diagram above the figures shows the experimental protocol of neutrophil depletion. (A) Concentrations of protein in BALF, (B) number of neutrophils in blood and BALF, and (C) Cy5-BSA NPs in BALF with or without the ip injection of anti-Gr-1 antibody. Cy5-BSA NPs and Gr-1 antibody were iv and ip injected 4 h after LPS challenge, respectively. The samples were collected 20 h after the administration of NPs. All data represent means ± SD (n = 3–4 mice per group). N.D., not detected.

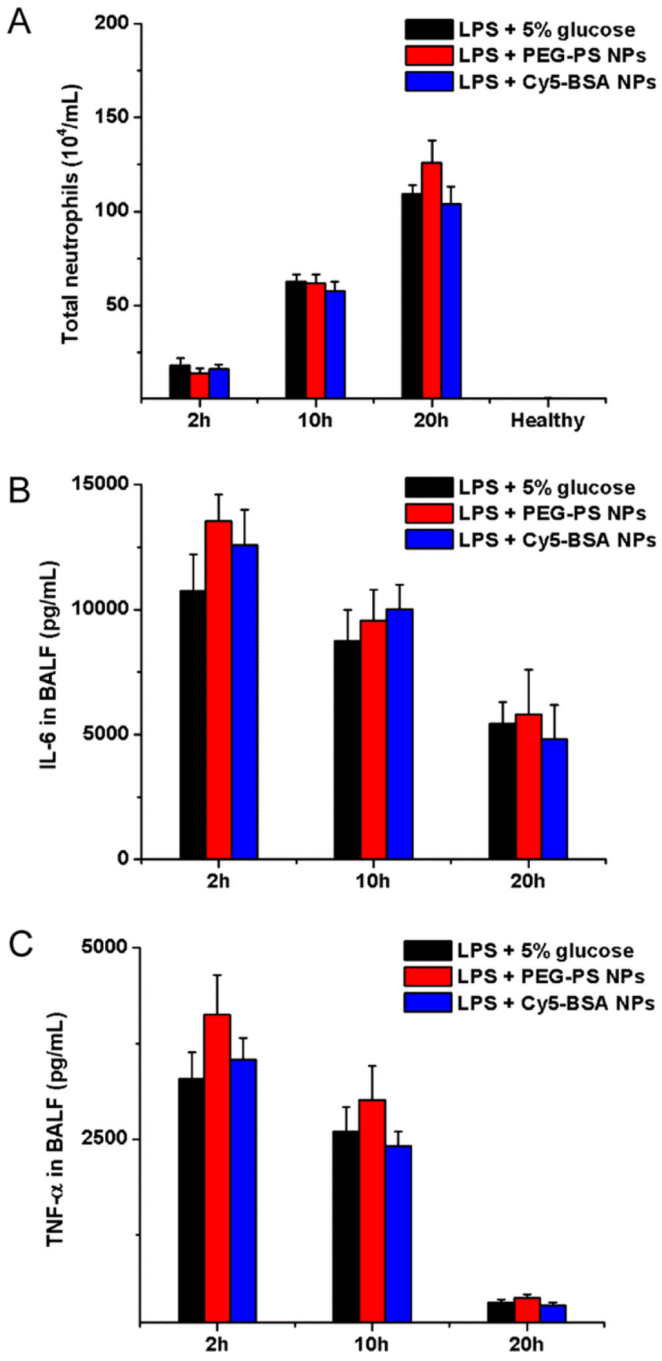

Figure 4.

Neutrophil uptake of albumin NPs does not alter neutrophil functions. (A) Number of neutrophils, concentrations of (B) IL-6 and (C) TNF-α in BALF after iv injection of 5% glucose, Cy5-BSA NPs, or PEG–PS NPs in mice 4 h after LPS challenge (8 mg/kg). All data represent means ± SD (3–4 mice per group).

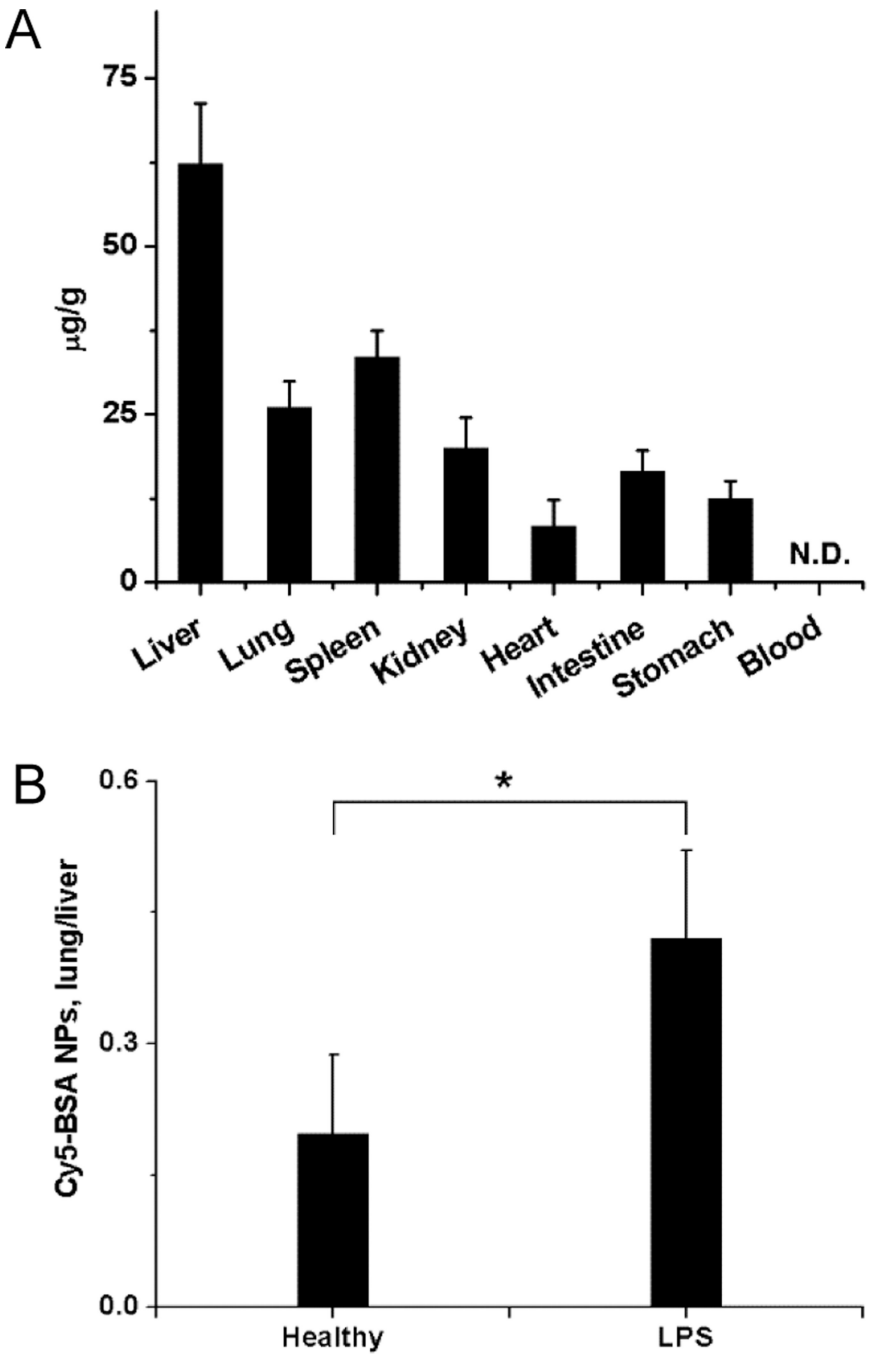

Figure 5.

Enhanced accumulation of albumin NPs in inflammatory lungs. (A) Biodistribution of albumin NPs in mice challenged with LPS. (B) Ratios of the amount of albumin NPs between lung and liver in mice challenged with LPS or without LPS (healthy mice). NPs were iv injected 4 h after LPS challenge. The samples were collected 20 h after the administration of NPs. All data represent means ± SD (n = 3–4 mice per group). Statistics were performed by a two-sample Student's t test (*P < 0.05). N.D., not detected.

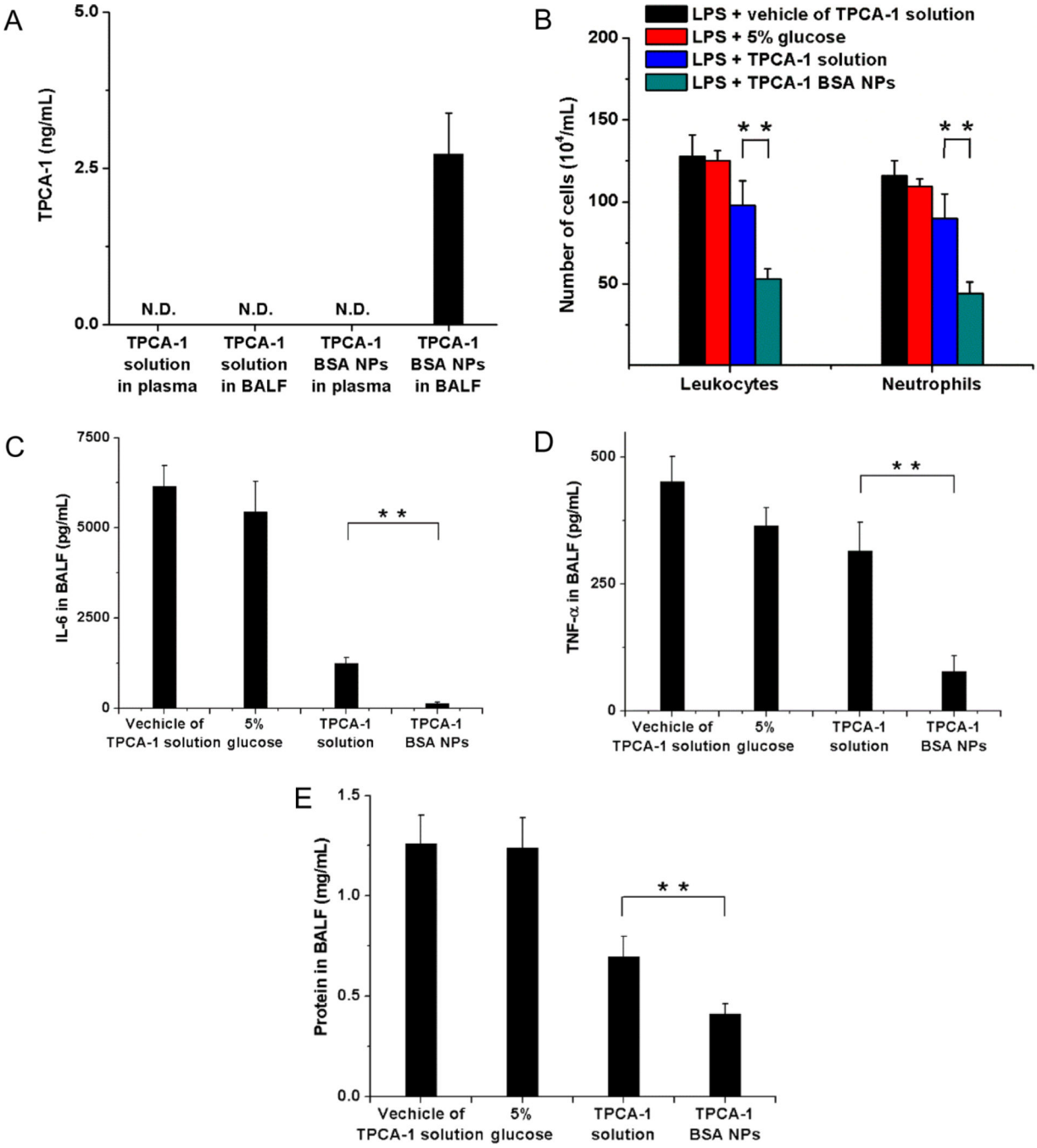

Figure 6.

Neutrophil-mediated delivery of TPCA-1 mitigates acute lung inflammation/injury. (A) Concentrations of TPCA-1 in plasma and BALF 20 h after iv injection of TPCA-1 loaded BSA NPs or TPCA-1 solution. N.D., not detected. (B) Numbers of leukocytes and neutrophils, concentrations of (C) IL-6, (D) TNF-α, and (E) proteins in BALF 20 h after iv injection of vehicle of TPCA-1 solution, 5% glucose, TPCA-1 solution or TPAC-1 BSA NPs in mice 4 h after LPS challenge (8 mg/kg). The dose of TPCA-1 was 8 mg/kg. All data

represent means ± SD (3–4 mice per group). Statistics were performed by a two-sample Student's *t* test (**$P < 0.01$).

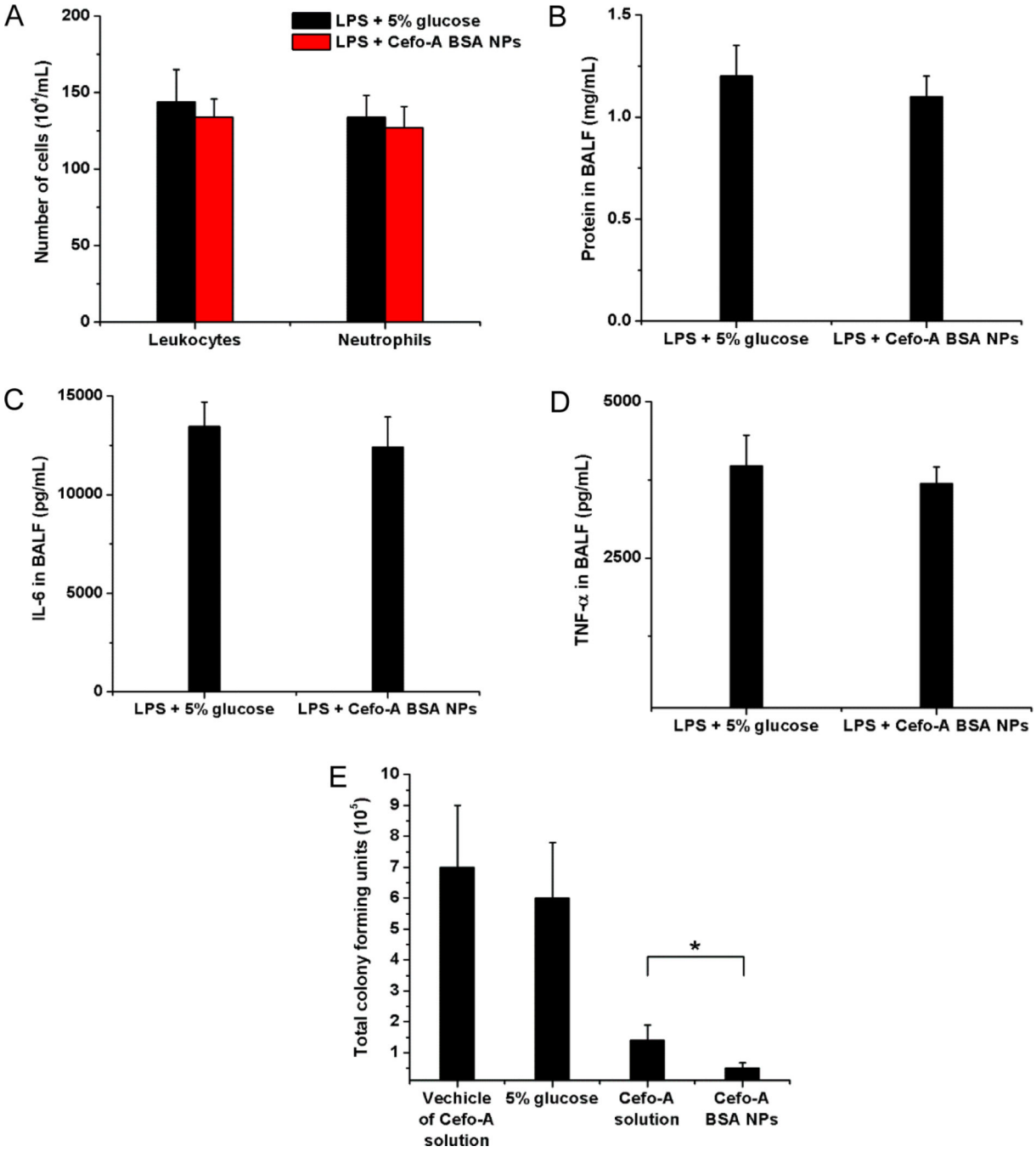

Figure 7.

Neutrophil-mediated delivery of antibiotic to infected lungs. (A) Number of leukocytes and neutrophils, (B) proteins, (C) IL-6, and (D) TNF-α in BALF after iv injection of 5% glucose and Cefo-A BSA NPs (25 mg/kg) in mice 12 h after intratracheal (it) LPS challenge (8 mg/kg). Samples were collected 12 h later. (E) Total colony forming units of *P. aeruginosa* in BALF after iv injection of 5% glucose, vehicle of Cefo-A solution, Cefo-A solution (25 mg/kg) and Cefo-A BSA NPs (25 mg/kg) in mice 12 h after *P. aeruginosa* infection (1×10^6

cfu/mL, 40 μL per mouse). Samples were collected 12 h later. All data represent mean ± SD (3–4 mice per group). Statistics were performed by a two-sample Student's *t* test (*$P < 0.05$).